

# Mechanism of U Insertion RNA Editing in Trypanosome Mitochondria: The Bimodal TUTase Activity of the Core Complex

Gene-Errol Ringpis<sup>1</sup>, Inna Aphasizheva<sup>1</sup>, Xiaorong Wang<sup>2</sup>, Lan Huang<sup>2</sup>, Richard H. Lathrop<sup>3,4</sup>, G. Wesley Hatfield<sup>4</sup> and Ruslan Aphasizhev<sup>1\*</sup>

<sup>1</sup>Department of Microbiology and Molecular Genetics, University of California Irvine School of Medicine, B240 Medical Sciences I, Irvine, CA 92697, USA

<sup>2</sup>Department of Physiology and Biophysics, University of California, Irvine, CA 92697, USA

<sup>3</sup>Department of Informatics and Computer Science, University of California, Irvine, CA 92697, USA

<sup>4</sup>Institute for Genomics and Bioinformatics, University of California, Irvine, CA 92697, USA

Received 9 December 2009;  
received in revised form  
23 March 2010;  
accepted 25 March 2010  
Available online  
1 April 2010

Expression of the trypanosomal mitochondrial genome requires the insertion and deletion of uridylyl residues at specific sites in pre-mRNAs. RET2 terminal uridylyl transferase is an integral component of the RNA editing core complex (RECC) and is responsible for the guide-RNA-dependent U insertion reaction. By analyzing RNA-interference-based knock-in *Trypanosoma brucei* cell lines, purified editing complex, and individual protein, we have investigated RET2's association with the RECC. In addition, the U insertion activity exhibited by RET2 as an RECC subunit was compared with characteristics of the monomeric protein. We show that interaction of RET2 with RECC is accomplished via a protein–protein contact between its middle domain and a structural subunit, MP81. The recombinant RET2 catalyzes a faithful editing on gapped (precleaved) double-stranded RNA substrates, and this reaction requires an internal monophosphate group at the 5' end of the mRNA 3' cleavage fragment. However, RET2 processivity is limited to insertion of three Us. Incorporation into the RECC voids the internal phosphate requirement and allows filling of longer gaps similar to those observed *in vivo*. Remarkably, monomeric and RECC-embedded enzymes display a similar bimodal activity: the distributive insertion of a single uracil is followed by a processive extension limited by the number of guiding nucleotides. Based on the RNA substrate specificity of RET2 and the purine-rich nature of U insertion sites, we propose that the distributive +1 insertion creates a substrate for the processive gap-filling reaction. Upon base-pairing of the +1 extended 5' cleavage fragment with a guiding nucleotide, this substrate is recognized by RET2 in a different mode compared to the product of the initial nucleolytic cleavage. Therefore, RET2 distinguishes base pairs in gapped RNA substrates which may constitute an additional checkpoint contributing to overall fidelity of the editing process.

© 2010 Elsevier Ltd. All rights reserved.

Edited by J. Karn

Keywords: *Trypanosoma*; mitochondria; RNA editing; TUTase; RNAi

\*Corresponding author. E-mail address: [ruslan@uci.edu](mailto:ruslan@uci.edu).

Abbreviations used: rRNA, ribosomal RNA; gRNA, guide RNA; RECC, RNA editing core complex; TUTase, terminal uridylyl transferase; dsRNA, double-stranded RNA; RET2, RNA editing TUTase 2; MEAT1, mitochondrial editosome-like complex-associated TUTase 1; RNAi, RNA interference; UTP, uridine triphosphate; ssRNA, single-stranded RNA; rRET2, recombinant RET2; iCODA, RNAi resistant genes via computationally optimized DNA assembly; MD, middle domain; TAP, tandem affinity purification; qRT-PCR, quantitative RT-PCR; WT, wild type; NTD, N-terminal domain; CTD, C-terminal domain; LC–MS/MS, liquid chromatography–tandem mass spectrometry (LC–MS/MS); Pol  $\beta$ , polymerase  $\beta$ ; EDTA, ethylenediaminetetraacetic acid; TEV, tobacco etch virus; IP, immunoprecipitation.

## Introduction

The mitochondrial genome of kinetoplastids (kinetoplast DNA, kDNA) represents one of the most complex DNA structures found in nature. The kinetoplast is a dense catenated network of ~50 maxicircles and ~10,000 minicircles. Maxicircles, ranging from 20 to 40 kb, encode conventional mitochondrial genes such as ribosomal RNAs (rRNAs) and subunits of respiratory complexes.<sup>1</sup> Twelve of the 18 protein-coding transcripts require posttranscriptional uridine insertion/deletion editing to generate translation-competent mRNAs.<sup>2-4</sup> These changes correct frameshifts, create start and stop codons, and, for some transcripts, generate large portions of their open reading frames.<sup>5-7</sup> Editing is directed by short (~60 nt) trans-acting guide RNAs (gRNAs) encoded primarily in the minicircles<sup>8</sup> or, in the case of subunit 2 of cytochrome oxidase, by a cis-interacting element located in the 3' untranslated region.<sup>9</sup>

The endonucleolytic, exonucleolytic, nucleoside transfer, and ligation activities are catalyzed by the ~1.2-MDa RNA editing core complex (RECC), also referred to as the 20S editosome or L-complex, which consists of ~20 polypeptides (reviewed in Refs. 10-12). The nomenclature of editing complexes and proteins proposed in Simpson *et al.*<sup>13</sup> has been

adopted here. In *Trypanosoma brucei*, three forms of RECC are distinguished by association with distinct RNase III-type endonucleases, REN1, REN2, and REN3, which are proposed to cleave at U deletion,<sup>14</sup> U insertion,<sup>15</sup> and cis-guided editing<sup>16</sup> sites, respectively (Fig. 1). Additional compositional differences among the RECC's include structural proteins (MP41, MP47, and MP49) and the exclusive presence of REX1 in the U deletion RECC1.<sup>16,17</sup> Although only RECC1 is presumed to be active in the U deletion editing, each RECC variant contains the components of both U insertion and U deletion pathways. These enzymatic cascades are mediated by spatially separate trimeric subcomplexes consisting of (1) a terminal uridylyl transferase (TUTase) or 3'-5' U-specific exonuclease, (2) a C2H2 zinc finger scaffolding protein, and (3) an RNA ligase.<sup>18</sup> Editing is initiated by mRNA cleavage immediately upstream of the "anchor" duplex formed between the gRNA 5' region and the preedited mRNA. Resultant 5' and 3' mRNA cleavage fragments are thought to be bridged by gRNA. For U deletion, unpaired Us are removed by either REX1 or REX2 exonucleases.<sup>19,20</sup> The postcleavage U insertion site represents a gapped double-stranded RNA (dsRNA) in which the 5' mRNA cleavage fragment terminates with a hydroxyl group, while the 3' cleavage fragment is 5'-phosphorylated (Fig. 1). Uracils are inserted by RNA editing TUTase 2

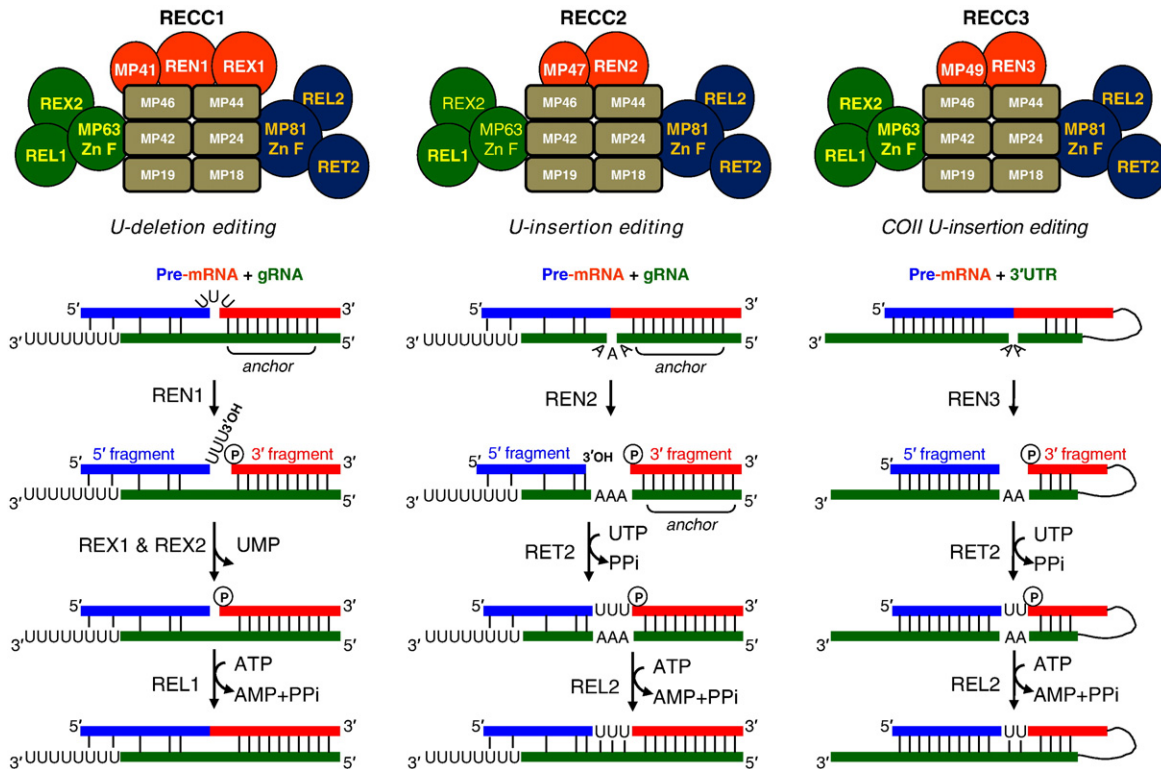


**Fig. 1.** Schematic representation of the U deletion (left), U insertion (middle), and cis editing (right) enzymatic cascades catalyzed by RECC1, RECC2, and RECC3, respectively. U insertion and U deletion subcomplexes are depicted in blue and green, respectively. MP, mitochondrial protein; REX, RNA editing exonuclease; REN, RNA editing endonuclease; REL, RNA editing ligase; RET, RNA editing TUTase; UTR, untranslated region; anchor, 5- to 15-nt-long double-stranded region formed by the 5' portion of the gRNA and preedited mRNA. Initial endonucleolytic mRNA cleavage occurs at the first unpaired nucleotide upstream of the anchor.

(RET2) according to the number of guiding purine nucleotides. Finally, the cleavage fragments are religated by editing ligases REL1 and REL2, producing an mRNA that is complementary to the gRNA.

In addition to RET2, two other mitochondrial TUTases are known in trypanosomes: RET1, which interacts with multiple complexes (reviewed in Ref. 11) to uridylylate gRNAs,<sup>21</sup> rRNAs,<sup>22,23</sup> and mRNAs,<sup>23–25</sup> and mitochondrial editosome-like complex-associated TUTase 1 (MEAT1), which interacts with an RECC-like complex, but also exists as an unassociated protein.<sup>26</sup> In contrast, RET2 is maintained only as a subunit of the U insertion subcomplex and is the sole nucleotidyl transferase of the RECC (Fig. 1). RET2 binds to the core complex via direct contact with MP81 zinc finger protein,<sup>27,28</sup> and its RNA interference (RNAi) knockdown in insect form parasites<sup>29</sup> or gene knockout in bloodstream form parasites<sup>30</sup> results in a severe growth inhibition. Loss of RET2 abolishes U insertion activity and decreases REL1 and MP81 protein levels but has no effect on the U deletion activity or the overall RECC integrity.<sup>29</sup>

U insertion editing is a unique method of transferring genetic information that does not rely on template-dependent nucleic acid polymerization, often allowing guanosine-residue-guided U insertion.<sup>28,29</sup> The uridine specificity is determined by RET2's intrinsic selectivity for uridine triphosphate (UTP)<sup>30</sup> and not by the nature of the guiding nucleotides. Recombinant RET2 is exclusively UTP specific and predominantly adds one uracil to a single-stranded RNA (ssRNA) terminating with adenine or guanine at the terminal base, but is virtually inactive on ssRNAs with Us at the 3' end.<sup>28,31</sup> However, faithful insertion editing of a synthetic precleaved editing substrate<sup>32</sup> has been shown using editing complexes purified to various degrees<sup>32–34</sup> and recombinant RET2 (rRET2)<sup>30</sup> (reviewed in Refs. 11 and 35). Therefore, specificity for a gapped dsRNA appears to be a key factor contributing to the overall fidelity of U insertion editing.

To understand the contributions of RET2's intrinsic properties and those conferred by its association with RECC, we investigated structural elements responsible for complex recruitment and enzymatic properties exhibited by RET2 as an RECC subunit and as an individual protein. By creating RNAi-based knock-in [iCODA (RNAi resistant genes via computationally optimized DNA assembly)<sup>26</sup>] cell lines of insect (procyclic) *T. brucei* and analyzing the activities of the purified RECC and the rRET2 on various RNA substrates, we show that interaction of RET2 with RECC is accomplished via a protein-protein contact between its middle domain (MD) and MP81 protein. The reaction catalyzed by rRET2 on gapped (precleaved) dsRNA substrates requires an internal monophosphate and is limited to insertion of three Us. Purified RECC does not require an internal phosphate and is capable of filling gaps similar to the longest ones observed *in vivo*. Despite moderate differences in catalytic efficiency, individual and RECC-embedded

enzymes display a similar bimodal activity: the distributive insertion of a single uracil is followed by a processive gap-filling reaction. We propose that the +1 insertion, which creates a substrate for the processive reaction, is likely followed by dissociation of RECC from RNA substrate. Upon base-pairing of the +1U-extended 5'-cleavage fragment with a guiding nucleotide, this substrate is recognized by RET2 in a different mode compared to the product of the initial nucleolytic cleavage. Therefore, prior to processive U insertion, RET2 distinguishes base pairs in gapped RNA substrates, which may be an additional checkpoint contributing to overall fidelity of the editing process. It is possible that the lack of +1U base-pairing would create a substrate for the 3'-5' U-specific exonuclease REX2 acting as a proofreading enzyme within the U insertion site. This hypothesis rationalizes an evolutionary pressure to maintain U deletion activity within RECC2 and RECC3, which are dedicated to U insertion sites (Fig. 1).

## Results

### Functional RNAi complementation and isolation of the active RET2 complex

To determine the protein module responsible for docking into the RECC and to assess the effects of RECC incorporation on RET2's catalytic parameters, we have further developed the iCODA technology<sup>26</sup> to enable affinity purification of WT and mutated proteins from a genetic background lacking the endogenous RET2 (Fig. 2). This methodology was previously employed to address potential RNAi off-targeting in knockdown studies of MEAT1.<sup>26</sup> As diagrammed in Fig. 2, RET2 knockdown was performed by cloning a fragment corresponding to positions 41–545 of the RET2 gene between opposing T7 RNA polymerase promoters and *tet* operators within the p217-177 vector.<sup>39</sup> The RET2 knock-in was accomplished by inducible coexpression of the RNAi-resistant gene that contained at least one silent mutation per 12 bp within the RNAi-targeted region. A C-terminal tandem affinity purification (TAP) tag<sup>40</sup> was also incorporated to allow affinity purification of RET2-iCODA protein from cells depleted of the endogenous protein.

While RET2 RNAi knockdown caused growth inhibition after ~80 h of induction, no significant changes in division time were observed for cells coexpressing the RNAi cassette and RET2-iCODA protein. Western blotting analysis demonstrated a depletion of the endogenous RET2 by RNAi and inducible expression of RET2-iCODA, which indicates a functional RNAi rescue (Fig. 3a). To verify unaltered levels of mitochondrial RNAs in RET2-iCODA/RNAi cells, quantitative RT-PCR (qRT-PCR) was used to measure the relative abundances of select never-edited, three preedited, and corresponding edited mRNAs (Fig. 3b). While the

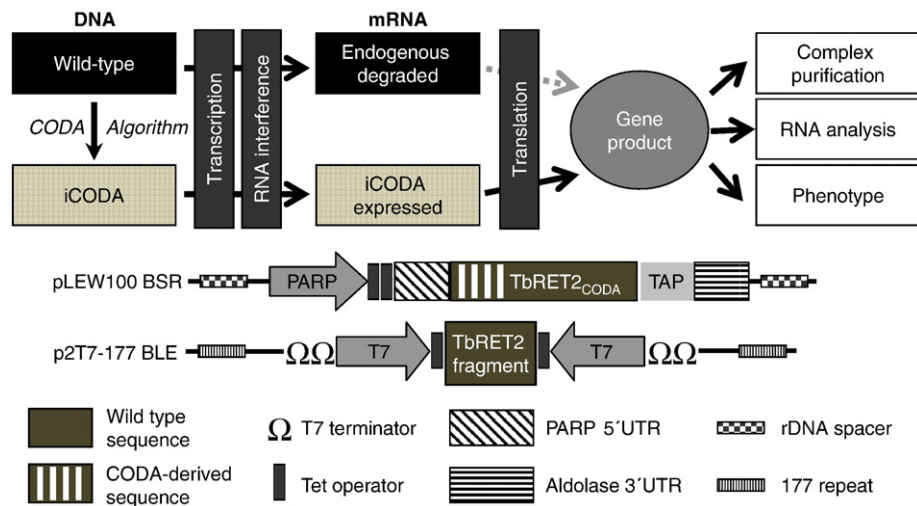


**Fig. 2.** Schematic representation of iCODA, an RNAi-based inducible knock-in strategy in the procyclic form of *T. brucei*. Silent mutations (at least one per 12 bp) were introduced into the RET2 gene region targeted by RNAi to minimize potential effects on translation<sup>36</sup> and to prevent transcript targeting by the RNAi machinery. The coexpression of both RET2-iCODA protein and RET2 RNAi cassette is controlled by tet operators positioned downstream of a procyclic acidic repetitive protein promoter (PARP), which is recognized by RNA polymerase I, and T7 RNA polymerase promoters, respectively. Coexpression is performed in *T. brucei* strain 29-13 that constitutively expresses T7 RNA polymerase and *tet* repressor.<sup>37</sup> BSR, blasticidin resistance gene; BLE, phleomycin resistance gene; 177 repeat, transcriptionally silent 177-bp satellite repeat sequence;<sup>38</sup> rDNA spacer, transcriptionally silent spacers between rRNA genes.

endogenous RET2 mRNA was degraded by more than 90%, all mitochondrial mRNAs tested remained virtually unaffected, confirming intact U insertion editing activity in RET2-iCODA/RNAi cells.

The presence of both endogenous and TAP-tagged RNA editing ligases in RECC purified from *Leishmania tarentolae*<sup>29</sup> and *T. brucei*<sup>18</sup> suggested that at least some components may be present in more than one copy per complex. To confirm RET2-iCODA incorporation into RECC and to assess its stoichiometry within RECC, we purified complexes from cells overexpressing TAP-tagged structural subunit MP63, WT RET2 and RET2-iCODA, and cells coexpressing RET2-iCODA and RET2 RNAi. The resultant protein profiles (Fig. 3c) and self-adenylation signals of RNA editing ligases (Fig. 3d, upper panel) were nearly identical among all three RET2 preparations, demonstrating equal complex integration of RET2-iCODA. Immunoblotting also showed similar levels of tagged RET2 polypeptides, which are slightly larger because of residual tags as compared to the endogenous RET2 in MP63-purified complex (Fig. 3d, bottom panel). Most importantly, the lack of the endogenous RET2 in complexes purified from either high- or moderate-level expression systems (mhTAP and pLEW100, respectively) demonstrated that there is a single RET2 molecule per RECC.

Finally, to compare the *in vitro* U insertion activities of all three RET2 complexes, affinity-purified fractions were tested in a precleaved RNA editing assay.<sup>32</sup> Synthetic RNAs (5' fragment, 3' fragment, and gRNA) were annealed to form a gapped dsRNA mimicking an editing substrate in

which the mRNA-gRNA hybrid had already undergone endonucleolytic cleavage. No apparent differences in U addition to ssRNA substrate and U insertion into fully assembled precleaved editing substrates programmed for +2U insertion were found among respective complexes (Fig. 3e). To conclude, complex purified from RET2-iCODA/RNAi cells has activity similar to those purified from RET2-overexpressing cell lines.

### The MD is required for RET2 incorporation into the RECC

Superpositioning of the crystal structures of RET2<sup>30</sup> and the smallest known TUTase, TUT4,<sup>43</sup> revealed a compact MD (~110 amino acids) inserted within the RET2 N-terminal catalytic domain (NTD). The site of MD insertion is highly conserved among trypanosomal uridylyl transferases and noncanonical poly(A) polymerases, but the primary structures of MDs are highly divergent.<sup>11</sup> The deleterious effect of MD deletion on ssRNA-specific RET1 TUTase activity suggested that MDs may be functionally important.<sup>44</sup> Indeed, the presence of a divergent module within an otherwise conserved NTD suggests that the MD may act as a function-specific adaptor for the catalytic "bidomain" formed by the NTD and the C-terminal domain (CTD).<sup>30</sup> We hypothesized that the MD is required for binding to the zinc finger containing structural subunit MP81<sup>18,28</sup> and, therefore, RET2 docking into the U insertion subcomplex. To investigate the role of the MD in RET2-MP81 binding *in vivo*, we have replaced residues 151–264 with a Gly-Ser-Gly-Ser linker to accommodate an

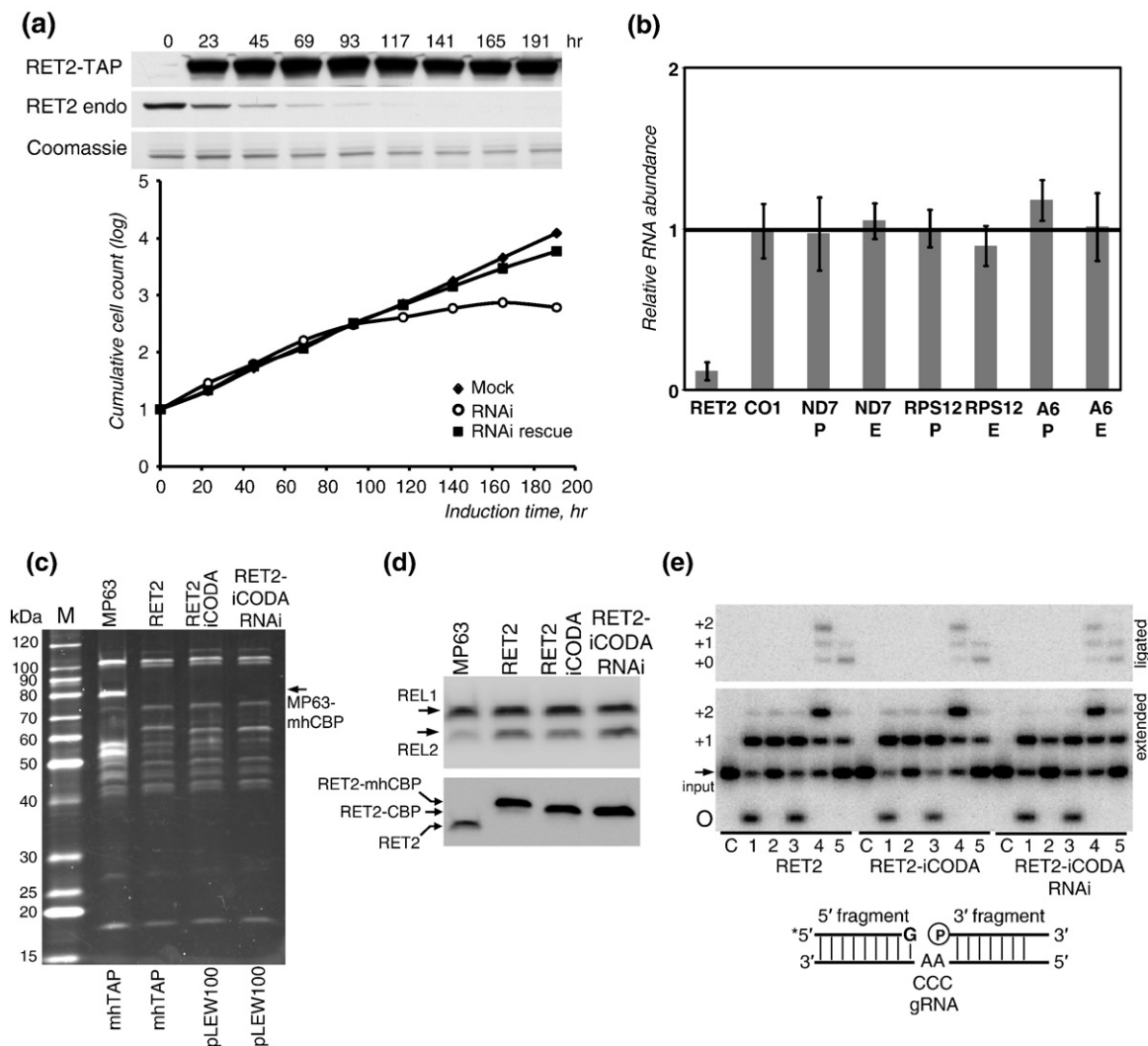


**Fig. 3.** Functional complementation of RET2 RNAi knockdown by coexpression of the RNAi-resistant transcript. (a) Growth kinetics of RET2-RNAi and RET2-iCODA/RNAi cell lines. Mock, uninduced RNAi cell; RNAi, tet-induced RNAi cells; RNAi rescue, tet-induced RET2-iCODA RNAi cells. Immunoblotting of endogenous and iCODA-derived RET2 in RNAi rescue cells is shown above the graph. (b) qRT-PCR analysis of mitochondrial mRNAs and endogenous RNAi-targeted RET2 transcript in RET2-iCODA/RNAi cells. RNA levels were normalized to  $\alpha$ -tubulin mRNA. P, preedited mRNA; E, edited mRNA. Error bars, standard deviation of three replicates. The thick line at 1 indicates no change in mRNA relative abundance; bars above and below represent an increase or decrease, respectively. (c) TAP-purified RECCs were separated on an 8–16% gradient SDS-PAGE gel and stained with Sypro Ruby. Cell lines and genetic constructs used for expression of TAP-tagged proteins are listed above and below the gel, respectively. The pLEW79-based mhTAP vector<sup>41</sup> was used for overexpression of MP63 structural protein and WT RET2. The pLEW100-BSR-based TAP vector<sup>42</sup> was used for expression iCODA-RET2. mhCBP, 6His tag plus calmodulin-binding peptide that remain on the tagged protein upon TEV protease cleavage. (d) TAP-purified complexes from (c) were analyzed by self-adenylation of RNA editing ligases in the presence of [ $\alpha$ -<sup>32</sup>P]ATP (top) and by Western blotting with anti-RET2 antibodies (bottom). (e) U insertion editing activity of TAP-purified complexes on precleaved editing substrates (diagrammed). Asterisk, radiolabeled 5' fragment. Top, ligated products; bottom, products of U addition to the 5' fragment. C, control, input RNA; 1, 5' fragment; 2, 5' fragment+gRNA; 3, 5' fragment+3' fragment; 4, full assembly (5' fragment+gRNA+3' fragment) with AA as guiding nucleotides; 5, full assembly with CCC as guiding nucleotides; circle, circularized 5' fragment.

~2.5 Å distance between the points of exit and return within the NTD. Coexpression of RET2 $\Delta$ M*D*-iCODA with RET2 RNAi induced a severe growth inhibition similar to that of RET2 RNAi, demonstrating that the deletion mutant was unable to compensate for knockdown of the endogenous protein (Fig. 4a and b).

Immunoblotting of cell lysates from parental 29-13,<sup>37</sup> RET2 $\Delta$ M*D*-iCODA, and RET2-iCODA cell lines demonstrated that mutated and full-length proteins were expressed at similar levels, while the endogenous RET2 was effectively depleted (Fig. 4b). Tandem affinity purification of complexes from RET2-iCODA and RET2 $\Delta$ M*D*-iCODA cells

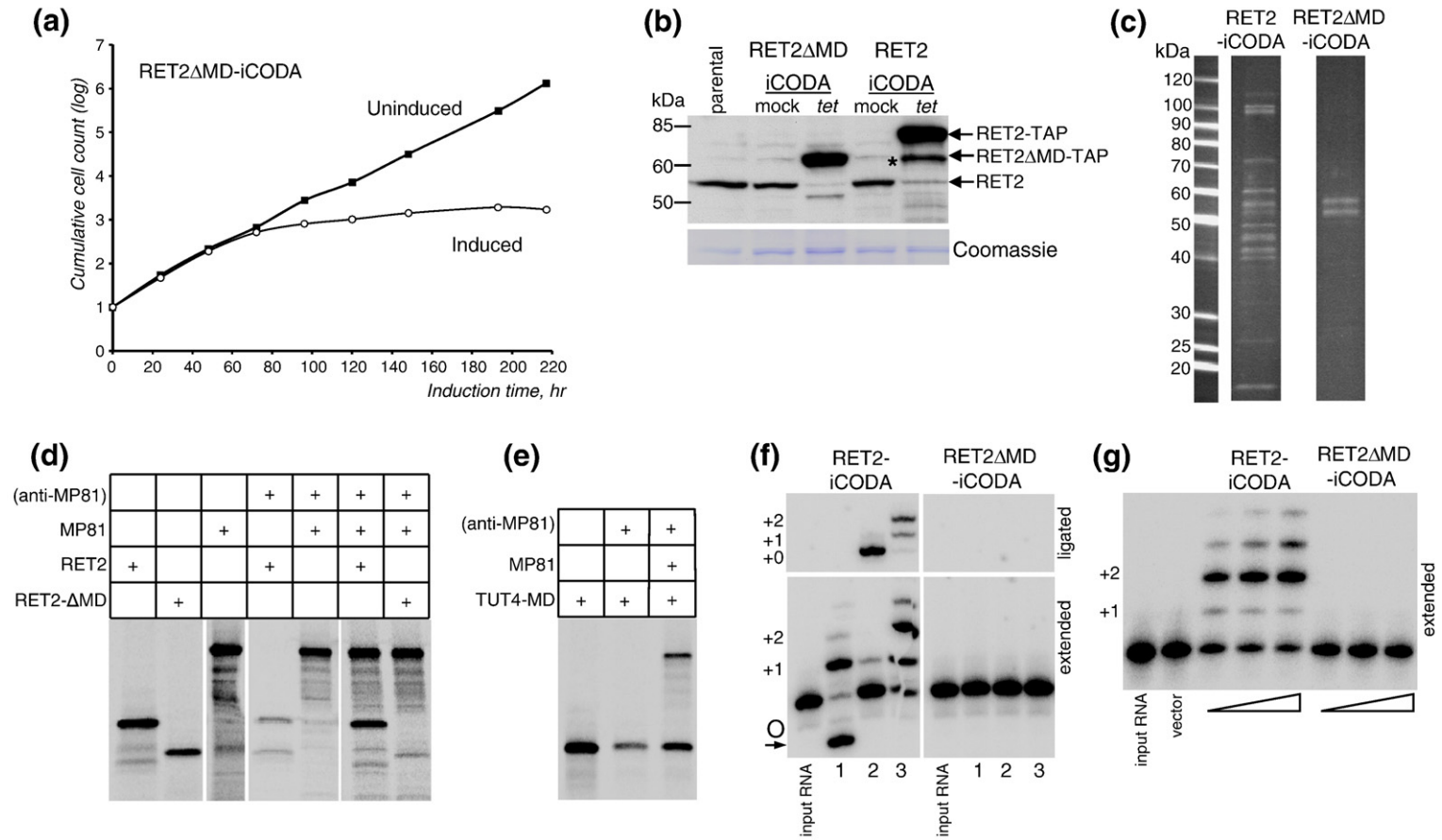


**Fig. 4.** Deletion of the MD disrupts RET2 incorporation into RECC- and RET2-mediated U insertion. (a) Growth kinetics of RET2ΔMD-iCODA/RNAi cells. (b) Western blotting analysis of RET2 knockdown and RET2ΔMD-TAP expression after 70 h of induction. RET2-iCODA/RNAi cells were analyzed alongside to demonstrate similar expression levels of RET2ΔMD and full-length RET2. The proteolysis product sporadically appearing in RET2-iCODA/RNAi cells is indicated by an asterisk. (c) TAP-purified complexes from RET2-iCODA/RNAi and RET2ΔMD-iCODA/RNAi cells were separated on an 8–16% gradient SDS-PAGE gel and stained with Sypro Ruby. (d) Coimmunoprecipitation of RET2 and RET2ΔMD with MP81 protein. All polypeptides were synthesized in the reticulocyte transcription–translation system in the presence of [<sup>35</sup>S] methionine. (e) Coimmunoprecipitation of *in vitro* synthesized <sup>35</sup>S-labeled MP81 and TbTUT4 TUTase with grafted RET2 MD. (f) U insertion and RNA ligase activities of TAP-purified fractions shown in (c). Protein amounts were normalized by Sypro-stained gel bands. The assay was carried out with 2 μl of purified fraction, 50 nM RNA, and 100 μM UTP for 1 h followed by 30 min incubation in the presence of 100 μM ATP. 1, 5' fragment; 2, +0 insertion substrate; 3, +2 insertion substrate. (g) U insertion activity of *in vitro* synthesized RET2 and RET2ΔMD proteins. The assay was carried out with 0.5, 1.0, and 3.0 μl of rabbit reticulocyte lysate (TnT Quick Coupled Transcription/Translation System, Promega) in the presence of 25 nM RNA substrate and 100 μM UTP for 1 h. Vector, expression plasmid pET15b (Novagen).

produced a typical RECC SDS gel profile for the former and two protein bands for the latter (Fig. 4c). To determine proteins associated with RET2 and RET2ΔMD, we subjected both affinity-purified fractions to sequential Lys-C and trypsin proteolysis and liquid chromatography–tandem mass spectrometry (LC–MS/MS) analysis. All 19 proteins that are currently viewed as subunits of the *T. brucei* core editing complex<sup>16,17,45</sup> have been identified in RET2-associated complex with high confidence (Table 1), including RET2 (42 peptides, 68% coverage) and MP81 (56 peptides, 66% coverage). The shorter RET2ΔMD bait protein produced 9 peptides (28% coverage), while only 4 peptides were detected for MP81 (7% coverage). The decreased MP81/RET2 peptide yield ratio demonstrates a significant loss of RET2-MP81 interaction *in vivo* and implicates the MD as an RECC docking interface.

We next examined the role of the MD in RET2:MP81 interaction *in vitro*. In agreement with affinity purification data, the stoichiometric coimmunoprecipitation of *in vitro* synthesized <sup>35</sup>S-labeled MP81 was observed with RET2 but not with RET2ΔMD protein (Fig. 4d). To address the possibility of conformational changes or folding problems caused by the MD deletion, we inquired whether grafting of the MD would confer MP81 binding properties to a different protein. We chose a nonmitochondrial TUTase, TUT4, as a recipient of the RET2's MD. Positions 130–132 of TbTUT4, which represent a short loop between the two enclosing β-strands that are nearly identical in RET2 and TUT4,<sup>43</sup> have been replaced with RET2's MD (positions 153–263, RET2 numbering). Although incubation of chimeric <sup>35</sup>S-labeled TbTUT4-MD protein with anti-MP81 antibody produced unusually high background, addition of MP81 into the binding reaction increased the efficiency of TbTUT4-MD immunoprecipitation by approximately twofold (Fig. 4e). Combined with negative coimmunoprecipitation of the full-length TbTUT4 and MP81 with anti-TUT4 or anti-MP81 antibody (not shown and Ref. 26), these data indicate a gain of MP81-binding function for the TbTUT4-MD protein. Collectively, our findings demonstrate that the MD is required for RET2 docking into the RECC via a direct contact with structural zinc finger protein MP81.

### The MD is essential for RET2 enzymatic activity

To analyze the effects of MD deletion on catalysis, we tested the ssRNA U addition and dsRNA U insertion activities of the full-length RET2 and RET2ΔMD affinity-purified fractions. The mRNA 5' cleavage fragment was used as a generic ssRNA substrate, while the precleaved editing substrate programmed for +2 insertion served as a model dsRNA (Fig. 4f). Taking into account the MS analysis of RET2 and RET2ΔMD affinity-purified fractions (Table 1), the complete lack of U insertion editing activity in the RET2ΔMD fraction was most likely caused by MD deletion, whereas the loss of RNA ligase activity is consistent with missing RNA ligases and most other editosome components. The detrimental effect of MD deletion on RET2 enzymatic activity was further confirmed using *in vitro* synthesized RET2 and RET2ΔMD proteins and precleaved RNA substrates (Fig. 4g).

To conclude, our data indicate that MD is required for both RECC docking and enzymatic activity of RET2. Although the MD deletion may have caused structural changes detrimental for MP81 binding and TUTase activity, available evidence suggests MD's direct involvement in these functions. The overexpression of RET2ΔMD in *T. brucei* produced no discernable phenotype, while a single-amino-acid mutation in the catalytic site (D97A) led to a dramatic growth inhibition (not shown). Apparently, the dominant-negative effect occurs only if the inactive protein associates with RECC. Finally, single-amino-acid changes along the putative RNA binding path extending across the MD lead to inhibition of RET2 activity, but not RECC incorporation (Ringpis *et al.*, submitted).

### RECC and rRET2 show distinct RNA substrate requirements and processivity *in vitro*

The order of RNA and UTP substrate addition has been shown to dramatically affect the processivity of LtRET1 TUTase,<sup>44</sup> which is capable of UTP polymerization without RNA, and the efficiency of the TbTUT4-catalyzed reaction.<sup>31</sup> Combined with crystallographic analysis of TbTUT4-UTP<sup>43</sup> and TbTUT4-UTP-UMP<sup>31</sup> complexes, these findings demonstrate that UTP can partially occupy the RNA binding site and compete with a polynucleotide substrate. The

**Table 1.** MS analysis of affinity-purified RET2 and RET2ΔMD complexes

		RET2				RET2ΔMD	
Protein	Peptides	Protein	Peptides	Protein	Peptides	Protein	Peptides
MP81	56	MP41	31	RET2	42	MP81	4
MP63	40	MP24	17	REX1	38	RET2	9
MP49	10	MP19	12	REX2	53		
MP47	35	MP18	10	REL1	32		
MP46	26	REN1	39	REL2	38		
MP44	30	REN2	38				
MP42	28	REN3	28				

Established components of the core editing complex (20S editosome) are listed.<sup>17,45</sup> The number of unique peptides identified by LC–MS/MS is indicated for each polypeptide.

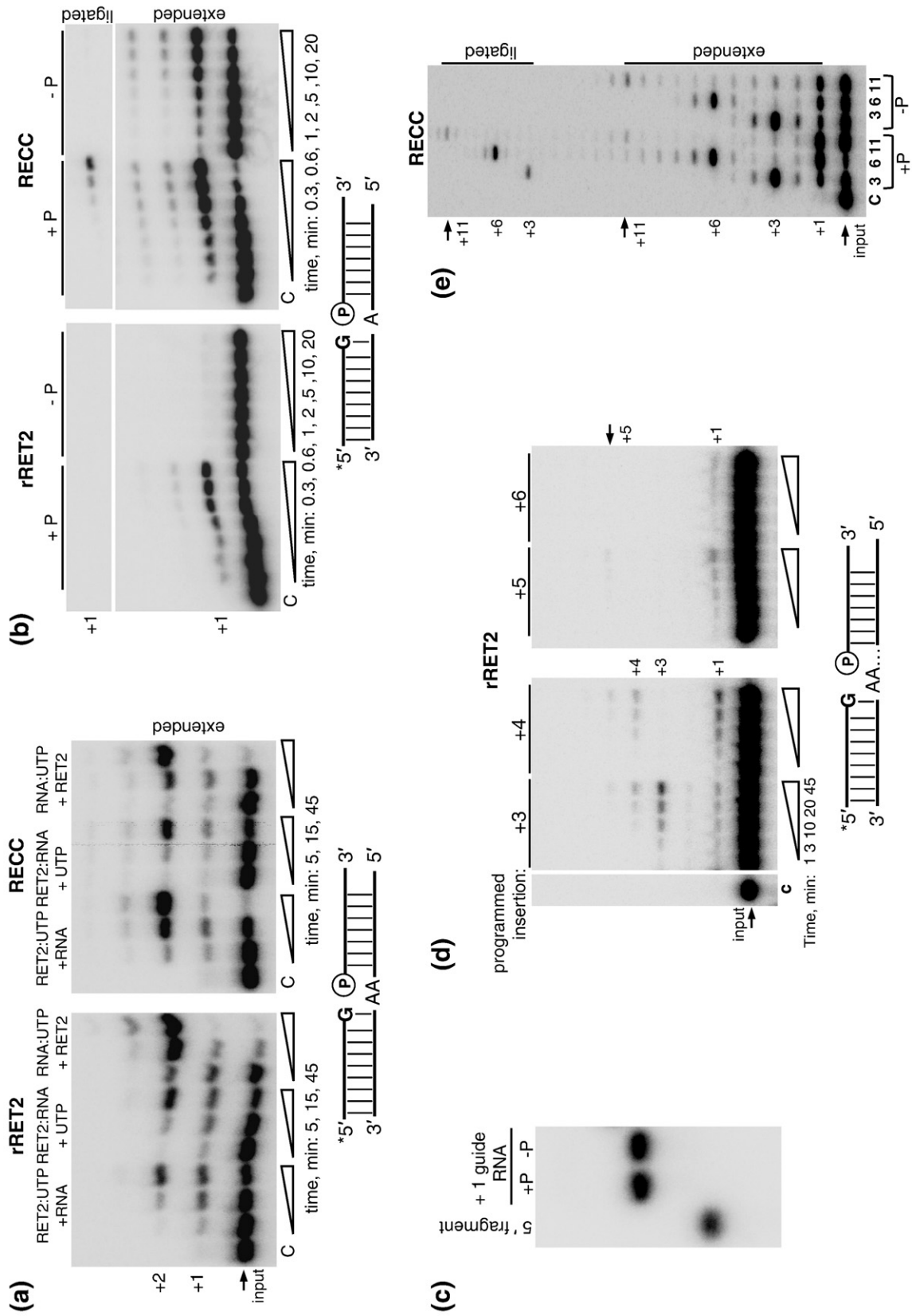


Fig. 5 (Legend on next page)

**Table 2.** Steady-state kinetic parameters of UTP incorporation by rRET2 and RECC

Enzyme	Substrate	$K_m$ , UTP ( $\mu\text{M}$ )	$k_{\text{cat}}$ ( $\text{min}^{-1}$ )	$k_{\text{cat}}/K_m$ ( $\text{min}^{-1} \text{M}^{-1}$ )
rRET2	0U	2.5 $\pm$ 1.9	0.02 $\pm$ 0.002	8.0 $\times 10^3$
RECC	0U	0.4 $\pm$ 0.05	0.04 $\pm$ 0.0004	1.0 $\times 10^5$
rRET2	1U	12.6 $\pm$ 3.2	0.20 $\pm$ 0.0007	1.6 $\times 10^4$
RECC	1U	20.8 $\pm$ 5.9	0.09 $\pm$ 0.005	4.0 $\times 10^3$

opposite situation of RNA substrate partially occupying the UTP binding site also seems possible based on TbTUT4-UpU structure<sup>31</sup> and close positioning of RET2's UTP binding site and UTP-UMP binding site (site B), which is likely involved in RNA substrate coordination.<sup>30</sup> To assess the effect of the order of substrate addition on rRET2- and RECC-catalyzed U insertions, the reactions were started by the addition of RNA, UTP, or protein to preincubated protein plus UTP, protein plus RNA, and RNA plus UTP mixtures, respectively. Time-course analysis showed less efficient U insertion when rRET2 was preincubated with either substrate compared to the reaction initiated by enzyme addition (Fig. 5a, left panel), which is consistent with competition between the two substrates for the RET2 catalytic site. However, the efficiency of the RECC-catalyzed reaction was unaffected by the order of substrate addition. Although we have not been able to accurately measure an apparent  $K_d$  for RET2 and RECC for technical reasons, these observations indirectly suggest that RECC's higher affinity for RNA overcame competition with UTP for the RNA binding site (Fig. 5a, right panel).

RET2, a member of the DNA polymerase  $\beta$  (Pol  $\beta$ ) superfamily of nucleotidyl transferases,<sup>46</sup> recognizes a dsRNA that resembles DNA Pol  $\beta$ 's gapped DNA substrate during nucleotide excision repair.<sup>47</sup> The 5'-monophosphate at the 3' fragment is critical for DNA binding by the purified Pol  $\beta$  whose gap-filling capacity *in vitro* is limited to 3 to 4 nt.<sup>48</sup> This constraint is imposed by a proximity requirement between the 5' fragment's hydroxyl group and the internal monophosphate. The monophosphate moiety, which participates in the post-U insertion ligation of 5' and 3' fragments,<sup>32</sup> is also critical for rRET2's activity on dsRNA with a 2-nt gap.<sup>26</sup> To minimize proximity effects, we have compared rRET2 and RECC activities on RNA substrates bearing a single-nucleotide gap. As expected, rRET2 efficiently inserted one uracil residue

into editing substrates possessing a 5'-phosphorylated 3' cleavage fragment, but was inactive in the absence of an internal monophosphate (Fig. 5b, left panel). In contrast, RECC-catalyzed +1U insertion was equally efficient on substrates possessing or lacking the 5'-monophosphate group. As expected, the ligation reaction was completely blocked for the latter substrate (Fig. 5b, right panel).

To ensure that the +1U insertion occurs within a dsRNA and not with unassembled 5' fragment, the annealed tripartite substrates with 5'-phosphorylated or dephosphorylated 3' fragments were separated on a native gel alongside with the 5' fragment (Fig. 5c). In conclusion, recognition of a monophosphate appears to be a conserved feature of Pol- $\beta$  family members acting on double-stranded gapped substrates. In RECC, lack of this positive contribution is likely compensated for by its higher affinity for RNA, which is consistent with order-of-addition experiments (Fig. 5a).

Previous studies using partially purified mitochondrial extracts,<sup>34</sup> purified editing complexes,<sup>28,33</sup> and rRET2<sup>30</sup> have demonstrated guided U insertions of up to three uracil residues. However, U insertions *in vivo* range from a single nucleotide to 12 uridines.<sup>49</sup> Therefore, we next determined whether rRET2 and RECC can act on longer gaps. Recombinant RET2 efficiently filled gaps of up to 3 nt, but its activity declined sharply on editing substrates programmed for more insertions (Fig. 5d). This observation is consistent with a monophosphate requirement, suggesting that, similar to DNA Pol  $\beta$ , the 3'-hydroxyl must be tethered in close proximity (1- to 3-nt gap) to the monophosphate group to be recognized by the enzyme. In contrast, the RECC-embedded RET2 achieved up to 11 guided U insertions irrespective of the phosphate presence (Fig. 5e). Thus, association with RECC stimulates RET2's processivity and enables filling of longer gaps in dsRNA substrates.

### Distributive insertion of the first U generates a substrate for a processive gap filling

We have noticed that a single uracil is not only inserted with similar efficiency into a +1 programmed substrate by both rRET2 and RECC (Fig. 5b and Table 2), but the +1U is also a prominent product on dsRNAs with longer gaps.

**Fig. 5.** RECC incorporation increases RET2 RNA affinity and processivity. (a) Effect of the substrate addition order. Pre-cleaved editing assays were carried out with 20 nM rRET2 (left) and 2.8 nM RECC-embedded RET2 (concentration estimated by Western blotting with anti-RET2 antibody in reference to rRET2; right). Pre-cleaved RNA substrate programmed for +2 insertion and UTP were present at 100 nM and 100  $\mu\text{M}$ , respectively. C, control, input RNA. (b) Effect of the phosphate group at the 5' end of the 3' cleavage fragment. Reactions were performed as in (a) with substrates programmed for +1 insertion for indicated periods. Top, ligated products. Bottom, U insertion products. +P, 5'-phosphorylated 3' cleavage product; -P, 3' cleavage fragment with 5'-hydroxyl group. (c) Assembly of the pre-cleaved editing substrate. Annealed pre-cleaved RNA substrates from (b) were separated alongside the 5' cleavage fragment on a 10% acrylamide native Tris-Hepes gel. (d) Processivity of rRET2. U insertion assay was performed with 20 nM protein, 100  $\mu\text{M}$  UTP, and RNA substrates programmed for 3, 4, 5, and 6 U insertions for indicated periods. (e) Processivity of RECC-catalyzed U insertion reactions. Assays were performed for 45 min as in (d). RECC-embedded RET2 (2.8 nM) was incubated with radiolabeled 5' cleavage fragment, phosphorylated (+P) or nonphosphorylated (-P) 3' cleavage fragment and gRNAs with indicated gap sizes in the presence of 100  $\mu\text{M}$  UTP.

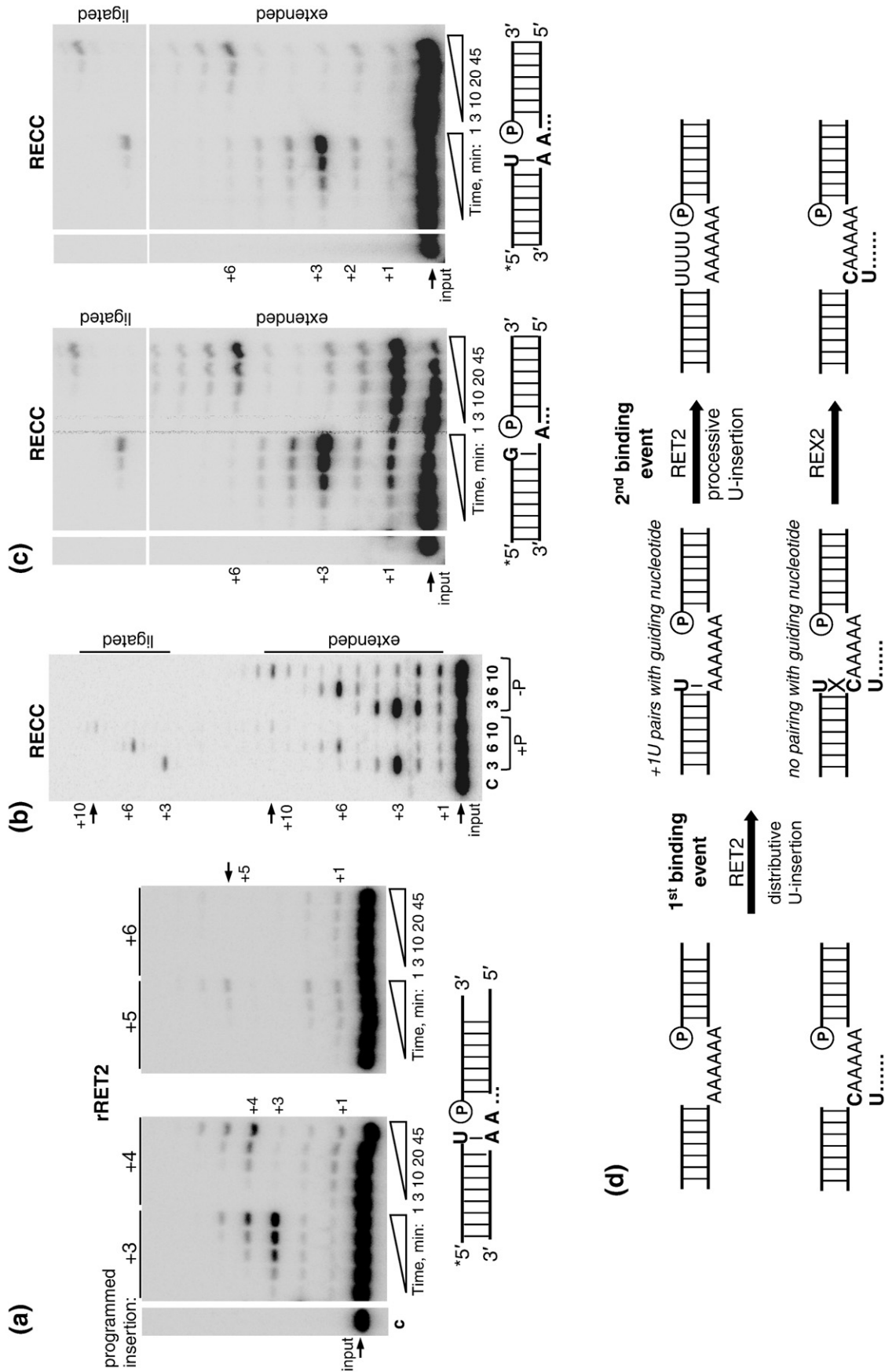


Fig. 6 (legend on next page)

It has also been shown that the partially purified editing complex adds a single U to a 5' cleavage product regardless of the base-pairing capacity with corresponding guiding nucleotide.<sup>34</sup> We hypothesized that a distributive +1 insertion acts as an additional specificity mechanism by which the presence of a correct base-pairing with gRNA is monitored: if +1 addition hybridizes with a guiding purine, the editing complex rebinds and catalyzes a processing gap filling.

It has been shown that TUT4<sup>31</sup> and MEAT1<sup>26</sup> TUTases prefer uracils at the terminal base of the ssRNA substrate, while RET2 prefers terminal purines.<sup>28,31</sup> This is expected, since endonucleolytic cleavage produces As or Gs as the terminal base in the 5' cleavage fragment in ~99% of all U insertion editing sites.<sup>49</sup> We first asked whether RET2's catalytic parameters in +1U insertion reaction are affected by its incorporation into RECC and the nature of the 3' nucleotide in the 5' fragment. The apparent  $K_m$  and rate constants of UTP incorporation were determined for dsRNA substrates programmed for a +1 insertion and G or U as terminal bases of the 5' cleavage fragment (Table 2). Moderate differences in catalytic efficiencies of rRET2 and RECC on both substrates suggest that neither the chemical nature of the terminal base nor complex association exert significant effects on +1U insertion activity.

We next inquired whether the capacity to fill longer gaps would be altered by the presence of a terminal U–A base pair in a 5' fragment–gRNA hybrid, which imitates a precleaved substrate following a single round of U insertion. The activity of the rRET2 was indeed stimulated by the presence of a terminal U residue not only yielding prominent +3 and +4 signals but also reaching +5 insertion (Fig. 6a). The RECC-catalyzed reaction was similar on substrates ending with G (Fig. 5d) or U (Fig. 6b) in terms of processivity and yield of guided products and was not affected by the lack of phosphate group. The prominent +1U insertion, however, was not observed on RNA substrates in which the 5' fragment already contained a uracil at the 3' end. To further strengthen this conclusion, the RECC-catalyzed U insertion was tested on both RNA substrates as a function of the reaction time (Fig. 6c). Apparently, the +1 is a predominant insertion to the purine-terminated 5' fragment and is more prominent on the longer 6-nt gap (Fig. 6c, left panel) likely because the shorter 3-nt gap is filled more efficiently. In the case of the 5' fragment

terminating with U, virtually no accumulation of +1 product was detected (Fig. 6c, right panel). These findings suggest that the RECC-embedded RET2 catalyzes a bimodal reaction: distributive addition of a single uracil to the 5' fragment and, upon hybridization of this residue to a guiding purine on the opposite strand, a processive filling of the gap according to the number of guiding nucleotides.

## Discussion

Here, we have determined a specific domain required for RET2 incorporation into RECC and compared enzymatic properties of monomeric and RECC-embedded RET2. We have utilized RNAi knockdown/knock-in cell lines of procyclic *T. brucei*, bacterial expression, and *in vitro* protein synthesis systems to obtain highly purified complexes and individual proteins. Activities of unassociated and RECC-bound RET2 were tested on synthetic RNA substrates that resemble intermediates of the U insertion reaction and allow incorporation of up to 11 uridine residues. While endonuclease, exonuclease, and RNA ligase activities are executed by two or more homologous enzymes, RET2 represents the only nucleotidyl transferase found in all variants of the core complex. Hence, a combination of a novel genetic system (iCODA) and an available X-ray crystal structure<sup>30</sup> presents a unique opportunity to determine whether association of editing enzymes into a stable complex alters their intrinsic substrate specificities and catalytic efficiencies. The iCODA methodology provided not only a means to study RET2 within the RECC context, but also established that a single RET2 molecule is present per complex. In contrast to dominant-negative approaches, the iCODA system proved to be of value for *in vivo* analysis of mutant proteins lacking domains required for complex association. In addition, the successful knock-in confirmed exquisite specificity of RNAi knockdown in *T. brucei*: introduction of a single mismatch per 12 bp into a synthetic gene was sufficient to confer an RNAi resistance to its transcript.

A pronounced sequence similarity between the N-terminal catalytic and C-terminal base-recognition domains of trypanosomal TUTases indicates conservation of these modules but provides few clues for the major differences in their enzymatic properties and capacities for specialized functions.

**Fig. 6.** Structure of the RNA substrate modulates RET2 activity. (a) Processivity of rRET2 on the gapped dsRNA assembled with 5' fragment that already contained a single uracil at the 3' end. U insertion assay was performed with 20 nM protein and 100  $\mu$ M UTP for indicated periods on RNA substrates programmed for +3, 4, 5, and 6 insertions. (b) Processivity of RECC on the RNA substrates, similar to those in (a), programmed for +3, +6, and +10 insertions. The assay was performed as in (a) with 2.8 nM RECC-embedded RET2 for 45 min. RNAs with indicated gap sizes were assembled with phosphorylated (+P) and nonphosphorylated (–P) 3' fragments. (c) Time-course of RECC-catalyzed U insertion on RNA substrates that imitate postcleavage (left) and post-1U insertion (right) intermediates programmed for +3 and +6 insertions. (d) A model of the U insertion editing reaction catalyzed by RECC2.

Interactions with binding partners are likely to be carried out by function-specific auxiliary domains, such as RET2's MD. Crystallographic studies of RET2 revealed that the NTD and CTD share a large interface, essentially creating a spherically shaped catalytic "bidomain."<sup>30</sup> The MD is inserted between two  $\beta$ -strands at the C-terminus of the NTD and folds out into the solvent while maintaining extensive interactions with the CTD. Positioning of the MD in respect to the catalytic cavity makes its contribution to UTP binding unlikely, but points to a potential role in RNA binding and/or protein-protein interactions. Indeed, MD deletion led to a complete enzyme inactivation and loss of association with the editing complex. The fact that *RET2 $\Delta$ MD* was expressed at a level comparable to that of the full-length gene suggests that the folding was not dramatically affected by the MD deletion. Grafting the RET2 MD into a topologically conserved site within TUT4 TUTase<sup>43</sup> led to a partial gain of interaction between the TUT4-MD chimeric protein and MP81, an established RET2 binding partner.<sup>18,45</sup> On the other hand, lack of TUTase activity in *RET2 $\Delta$ MD* indicates that the MD may be involved in both complex association and RNA binding.

The accuracy of U insertion into dsRNA is crucial for the overall fidelity of the editing process. Specificity for U is dictated by RET2's intrinsic selectivity for the uracil base<sup>30</sup> rather than by Watson-Crick base-pairing of the incoming UTP with guiding nucleotides.<sup>32,34</sup> The RET2 substrate is generated by the endonucleolytic mRNA cleavage, which leaves a phosphate group at the 5' end of the 3' fragment (Fig. 1). Consistent with previous study by Igo *et al.*<sup>32</sup> performed with mitochondrial extract enriched for editing activity, the phosphate is not required for U insertion by the RECC, but is essential for U insertion by monomeric RET2. This may reflect mechanistic similarities between RNA editing and base excision repair enzymes, but not their respective complexes. Indeed, gapped DNA substrates are generated by the AP endo-/exonuclease, which is homologous to the REX1/REX2 editing exonucleases, and then targeted by the DNA Pol  $\beta$ .<sup>20,50</sup> The DNA repair polymerase activity depends on 5' phosphate recognition<sup>48</sup> to processively extend the 5' fragment through the lesion but only if the gap does not exceed 4 to 5 nt, which matches the intrinsic processivity limit of monomeric RET2.

The phosphate group requirement for RET2-catalyzed reaction indicates that the double-stranded anchor with an internal 5'-monophosphate constitutes the RET2 binding site (Fig. 1). In case of RECC, the lack of phosphate dependence and capacity to fill longer gaps emphasizes the contribution of other subunit(s) to RNA binding. If RET2, as a core complex subunit, remains bound to the anchor duplex upon mRNA cleavage, the 3'-OH group of 5'-mRNA cleavage

fragment must be somehow positioned in the vicinity of the active center. For short gaps, the 3'-hydroxyl group may be held in sufficiently close proximity by one to three guiding nucleotides; hence efficient U insertion may not require additional RNA contacts outside of RET2. This hypothesis is consistent with very similar catalytic parameters for +1U insertion reactions catalyzed by RET2 and RECC (Table 2). For longer gaps, a greater entropy cost of bringing the 3'-OH group into the RET2 active site is likely to be compensated for by interactions with other RECC subunits. Structural protein MP81, which binds both RET2 and REL2 ligase<sup>18</sup> and has been shown to enhance RET2 activity *in vitro*,<sup>28</sup> is a primary candidate for providing these additional RNA binding contacts. Collectively, our data and earlier findings from the Stuart laboratory<sup>28,32,34</sup> suggest that complex association enhances RET2-catalyzed U insertion editing by optimal scaffolding of RNA substrates with gaps longer than 3 nt.

The endonucleolytic cleavage of typically purine-rich preedited mRNAs leaves As or Gs at the 3' end of the 5'-mRNA cleavage fragment. In mitochondrial extract, a single U insertion into a gapped dsRNA can be accomplished even if the opposite nucleotide in the gRNA (U or C) does not base-pair with the inserted uracil. The sequential +2 insertion, however, is inhibited.<sup>32</sup> Thus, although in the majority of U insertion editing sites U is first added to the mRNA fragment ending with purine, all sequential Us are added to RNA ending with uracil. We propose that the distributive +1 insertion acts as a "sampling mechanism" to ensure that a purine nucleotide occupies a base-pairing position in the opposite guiding strand. When the +1 extended product hybridizes to the guiding purine, RET2 recognizes the base pair of the opposite geometry in a different mode, which triggers processive U insertion. It remains to be elucidated whether the editing complex fully dissociates after +1U insertion and then rebinds in a different mode. The thermodynamic contribution of +1U insertion to stabilizing the gRNA-5' cleavage fragment binding is apparently negligible.<sup>34</sup> However, TUT4 structure and RET2 homology modeling imply that the RNA terminal base pair must enter the stacking interaction with the uracil base of the bound UTP.<sup>31</sup> Such interaction would favor UTP-3'-U stacking, which may stimulate RET2 processivity, while UTP-3'-purine stacking would be suboptimal for processive activity because of base translation. To conclude, the +1 insertion likely serves a dual function of verifying purine nucleotide occupancy in complementary gRNA and stimulating processive gap filling. In this scenario, an unpaired uracil may be removed by the U deletion activity upon RECC rebinding, which would explain an evolutionary pressure to keep components of the U deletion pathway in a core complex dedicated to U insertion (Fig. 1). It is plausible that REX2 acts on U insertion editing sites as a proofreading enzyme.

## Materials and Methods

### Cell cultures, RNAi, and RNA analysis

The RET2 RNAi expression plasmid was generated by cloning positions 41–545 of the RET2 gene into a p2T7-177 vector.<sup>39</sup> Clonal tetracycline-inducible RNAi cell lines were obtained by transfection of this construct into procyclic *T. brucei* strain 29-13<sup>37</sup> followed by selection by limiting dilution. RNAi was induced by the addition of tetracycline (1 µg/ml), and cells were diluted every 24 h to  $\sim 1 \times 10^6$ /ml. Isolation of total RNA and quantitative real-time PCR analysis of mitochondrial RNAs was performed as previously described.<sup>25,26,51</sup>

### iCODA

To generate the RNAi-resistant fragment of RET2*codA*, the following sequence was designed, assembled from oligonucleotides, cloned into pTOPO vector, and verified by sequencing:

```
5'-ATGTTGATGCACACAGCACCCCTGG
TTGCACATGAGGCTTAGTAGGTTGTT
TAGGCAGAGTCCACTTAGTTTGCCG
AGTACTAAACTTAACCCTAGTCCTG
ATCATTACGCAGTTTGGGGTAAGGC
AATTATGGCCGAAAATAATCGTAGG
GTAGGACCTGAGCACATGTTTCGTA
CAGCAATTAGGGCACAGCAGCAACT
TCAGGGTTTAGCTGATAAATGGACG
CCTGACGCAAAGGTGTACTGTTGTG
GTAGTATGGTGACGTACGGTCAGAT
GGAGTGGGGTAGTGATCTTGATTTA
GCATGTATGTTTGATGATCCATACC
CTAGTCATGAGGTTTCAGGCTAAGC
TACCGATAAGTTGTGGACAGTGATT
AAGCGCTACGTCCCACACTTGA
GGAACAATCTTTTAGGTCTGACTGA
AGCGCGTACACCAGTAGTAAAGTTG
AGGTTTGCTAACGATGAAAAGGTAG
CTAGGGCTAGGTACACACCATTGAG
CGAAGAAGAGGACCGTAAGGCAC
GTACAGCATTGCTTGATGTTAGG-3'.
```

To generate pLEW100-RET2-iCODA-TAP-BSR, the iCODA fragment was PCR-amplified with A222 and A223 primers. The recipient vector was amplified by inverted PCR from pLEW100-RET2-TAP-BSR with A220 and A221 primers. Both fragments were digested with HindIII, gel-purified, and ligated to replace the first 546 bp of the RET2 gene.

Clonal cell lines for RET2-iCODA/RET2 RNAi were generated by cotransfection of pLEW100-RET2-iCODA-TAP-BSR and p2T7-177-RET2 into procyclic *T. brucei* strain 29-13<sup>37</sup> and subsequent selection of cells resistant to blasticidin, phleomycin, hygromycin, and neomycin by limiting dilution. Concurrent RET2-iCODA-TAP expression and RET2 RNAi were induced by the addition of tetracycline at 1 µg/ml.

### Protein purification and *in vitro* synthesis

A RET2-iCODA gene lacking 21 codons at the 5' end (putative mitochondrial importation signal) was PCR-amplified and cloned into pET15b *Escherichia coli* expression vector. Recombinant RET2-iCODA was purified as

previously described.<sup>35</sup> For expression in *T. brucei*, the RET2 gene was cloned into pLEW79-BLE<sup>35</sup> and pLEW100-BSR vectors. Tandem affinity purification of RECC-embedded RET2 from whole-cell lysates ( $\sim 2 \times 10^{10}$  cells) was performed using a modified protocol.<sup>35</sup> Briefly, transgenic cell lines were grown in 2 liters of SDM-79 medium supplemented with 10% heat-inactivated fetal bovine serum, geneticin (G418; 50 µg/ml), hygromycin (50 µg/ml), hemin (10 µg/ml), and phleomycin (2.5 µg/ml) and/or blasticidin (10 µg/ml). Cells were induced with tetracycline (1 µg/ml), harvested after 48–72 h of induction, and centrifuged in a fixed-angle rotor at 5000g for 10 min. Subsequent purification was performed at 4 °C. The cell pellet was resuspended in 6 ml of extraction buffer [50 mM Tris-HCl (pH 7.6), 150 mM KCl, and 2 mM ethylenediaminetetraacetic acid (EDTA)]. NP-40 detergent was added to 0.3% plus 0.3 tablet of Complete™ (Roche) protease inhibitors. The extract was sonicated three times at 9 W for 10 s and then centrifuged at 100,000g for 15 min at 4 °C in a TLA 100 rotor (Beckman). The supernatant was harvested and the pellet was resuspended with 6 ml of extraction without NP-40 followed by another round of sonication. Pooled supernatants were filtered through a 0.45-µm membrane and incubated with 0.3 mL of IgG Sepharose resin (GE Healthcare) for 1 h. The material was transferred to a gravity-flow column and washed with 6 volumes of IgG binding buffer [25 mM Tris-HCl (pH 7.6), 150 mM KCl, 1 mM EDTA, and 0.1% NP-40] followed by 2 column volumes of tobacco etch virus (TEV) cleavage buffer (IgG binding buffer plus 1 mM DTT). The column was sealed and incubated overnight with gentle agitation with 1.5 ml of TEV cleavage buffer supplemented with 150 U of TEV protease and 0.02 tablet of Complete™ protease inhibitor. The IgG column was drained directly onto 300 µl of calmodulin resin. The IgG column was washed with an additional 3 ml of calmodulin binding buffer [25 mM Tris-HCl (pH 7.6), 150 mM KCl, 0.1% NP-40, 10 mM β-mercaptoethanol, 1 mM magnesium acetate, 1 mM imidazole, and 2 mM CaCl<sub>2</sub>] and the washes were also loaded on the calmodulin resin. The suspension was supplemented with 6 µl of 1 M CaCl<sub>2</sub> and then incubated with gentle agitation for 1 h. The suspension was transferred to a gravity-flow column and washed with 6 column volumes of calmodulin binding buffer. Complexes were then eluted with 25 mM Tris-HCl (pH 7.6), 150 mM KCl, 3 mM ethylene glycol bis(β-aminoethyl ether) *N,N'*-tetraacetic acid (EGTA), 1 mM EDTA, and 10% glycerol.

pET15b-based vectors were used to clone genes of interest under control of the T7 RNA polymerase promoter. <sup>35</sup>S-labeled proteins were synthesized with TNT Quick Coupled Transcription/Translation System (Promega). Briefly, 1 µg of plasmid DNA, 2 µl of [<sup>35</sup>S] methionine, and 40 µl of TnT Quick Master Mix were combined in a 50-µl reaction volume and incubated for 90 min at 30 °C.

### RNA substrates, enzymatic assays, and native gels

Editing ligase self-adenylation reactions were performed as described.<sup>35,52</sup> Pre-cleaved editing assays were carried out with 5–20 nM rRET2 or 2 µl of TAP-purified complexes or 0.5–2 µl of TNT lysate in 20 µl of 50 mM Hepes (pH 8.0), 10 mM MgCl<sub>2</sub>, 50 mM KCl, 1 mM DTT, and 100 µM UTP. RNA substrates<sup>35</sup> were assembled from chemically synthesized radiolabeled 5'-fragment, *in vitro* transcribed gRNA, and chemically synthesized 3'-fragment. Respective RNAs were mixed at 1:1.5:3 molar ratios in 20 mM Hepes-KOH buffer (pH 7.5) and 50 mM of KCl,

heated to 65 °C, and cooled to 4 °C for 30 min. The assembly of dsRNAs was verified by 10% native gel electrophoresis in 50 mM Tris–50 mM Hepes buffer (pH 7.8, without adjustment). RNA substrates were used in U insertion reactions at final concentration of 0.05–0.1 µM. For dsRNAs, the concentration of the 5' fragment was assumed. Reactions were terminated by the addition of 2 volumes of 0.5 M sodium acetate (pH 5.0), 10 mM EDTA, 0.1% SDS, and 2 µg of glycogen (Ambion). RNA was extracted with phenol–chloroform, precipitated with ethanol, and resuspended in 95% formamide, 0.05% bromophenol blue, 0.05% xylene cyanol FF, and 10 mM EDTA. The sample was denatured by heating at 80 °C for 2 min and analyzed on a 15% acrylamide–urea gel. Steady-state kinetic parameters of UMP incorporation were obtained with reaction times and UTP concentrations varying from 0.33 to 5 min and 0.5–150 µM, respectively.

### Western blotting and immunoprecipitation

Rabbit polyclonal antibodies against full-length rRET2 were affinity-purified on an antigen column. For Western blotting,  $\sim 3 \times 10^6$  cells were dissolved in SDS loading buffer, separated on an 8–16% gradient SDS-PAGE gel, and transferred to a nitrocellulose membrane. For coimmunoprecipitation assays, equal volumes of TnT lysates expressing <sup>35</sup>S-labeled proteins or containing empty vectors were combined for 15 min at 30 °C. Magnetic Protein G Dynabeads (Invitrogen) were coated with purified anti-MP81 monoclonal antibodies in immunoprecipitation (IP) buffer [20 mM Tris–HCl (pH 7.8), 150 mM NaCl, and 0.1% Triton X-100] and then saturated with bovine serum albumin (10 mg/ml) in IP buffer. For a single IP, 5 µl of bead suspension and 1 µg of total immunoglobulin were used. Beads were resuspended in 100 µl of IP buffer plus bovine serum albumin (10 mg/ml) and incubated with the 100-µl TnT reaction for 1 h at 4 °C with constant mixing. Beads were pelleted, washed three times with 1 ml of IP buffer for 15 min, resuspended in 1× SDS loading buffer, separated on an SDS-PAGE gel, and then transferred to a nitrocellulose membrane for visualization on a phosphor storage screen.

### Mass-spectrometric analysis by LC–MS/MS

LC–MS/MS was carried out by nanoflow reversed-phase liquid chromatography (RPLC) (Eksigent, Dublin, CA) coupled online to a linear ion trap (LTQ)-Orbitrap mass spectrometer (Thermo-Electron Corp). The LC analysis was performed using a capillary column (100 µm inside diameter×150 mm long) packed with Polaris C18-A resin (Varian Inc., CA); the peptides were eluted using a linear gradient of 2% to 35% B in 85 min at a flow rate of 300 nL/min (solvent A, 100% H<sub>2</sub>O–0.1% formic acid; solvent B, 100% acetonitrile–0.1% formic acid). A cycle of one full Fourier transform scan mass spectrum (350–2000 *m/z*, resolution of 60,000 at *m/z* 400) followed by 10 data-dependent MS/MS acquired in the linear ion trap with normalized collision energy (setting of 35%). Target ions already selected for MS/MS were dynamically excluded for 30 s.

Monoisotopic masses of parent ions and corresponding fragment ions, parent ion charge states, and ion intensities from the tandem mass spectra were obtained by using in-house software with Raw\_Extract script from Xcalibur v2.4. Following automated data extraction, resultant peak lists for each LC–MS/MS experiment were submitted to

the development version of Protein Prospector (University of California, San Francisco) for database searching similarly as described (X.W. and L.H., 2008, unpublished data). The *T. brucei* database v4† (09/01/2006, 8303 sequence entries) was used for database searching. Trypsin was set as the enzyme with a maximum of two missed cleavage sites. The mass tolerance for parent ion was set as ±20 ppm, whereas ±0.5-Da tolerance was chosen for the fragment ions. Chemical modifications such as protein N-terminal acetylation, methionine oxidation, N-terminal pyroglutamine, and deamidation of asparagine were selected as variable modifications during database search. The Search Compare program in Protein Prospector was used for summarization, validation, and comparison of results. To determine the expectation value cutoff that corresponds to a percent false positive (% FP) rate, we searched each project against a normal database concatenated with the reversed form of the database. An algorithm in Search Compare automatically plots the expectation values *versus* % FP rate for each search result. Based on these results, we chose an expectation value cutoff for all peptides corresponding to ≤0.025% FP. At this false-positive rate, false protein hits from decoy database were not observed. Positive protein identification was based on at least three peptides.

### Acknowledgements

We thank Ronald Etheridge and James Weng for help with qRT-PCR and complex purification and members of the Aphasizhev laboratory for stimulating discussions. We thank George Cross and Elisabetta Ullu for sharing trypanosomal strains and plasmids. Monoclonal antibody against MP81 was a kind gift of Ken Stuart. This work was supported by NIH grant AI064653 to R.A. G.R. was supported by the UCI Biomedical Informatics Training Program. All materials described in this article are available in accordance with the NIH grant policy on sharing of biomedical research resources. This manuscript has been approved by all authors. Authors declare no conflicts of interest or competing financial interests.

### Supplementary Data

Supplementary data associated with this article can be found, in the online version, at [doi:10.1016/j.jmb.2010.03.050](https://doi.org/10.1016/j.jmb.2010.03.050)

### References

1. Lukes, J., Guilbride, D. L., Votypka, J., Zikova, A., Benne, R. & Englund, P. T. (2002). Kinetoplast DNA network: evolution of an improbable structure. *Eukaryot. Cell*, **1**, 495–502.
2. Stuart, K., Allen, T. E., Heidmann, S. & Seiwert, S. D. (1997). RNA editing in kinetoplastid protozoa. *Microbiol. Rev.* **61**, 105–120.

† <http://www.genedb.org>

3. Stuart, K., Panigrahi, A. K., Schnaufer, A., Drozd, M., Clayton, C. & Salavati, R. (2002). Composition of the editing complex of *Trypanosoma brucei*. *Philos. Trans. R. Soc. London, Ser. B*, **357**, 71–79.
4. Simpson, L., Sbciego, S. & Aphasizhev, R. (2003). Uridine insertion/deletion RNA editing in trypanosome mitochondria: a complex business. *RNA*, **9**, 265–276.
5. Benne, R., Van den Burg, J., Brakenhoff, J., Sloof, P., Van Boom, J. & Tromp, M. (1986). Major transcript of the frameshifted *coxII* gene from trypanosome mitochondria contains four nucleotides that are not encoded in the DNA. *Cell*, **46**, 819–826.
6. Bhat, G. J., Koslowsky, D. J., Feagin, J. E., Smiley, B. L. & Stuart, K. (1990). An extensively edited mitochondrial transcript in kinetoplastids encodes a protein homologous to ATPase subunit 6. *Cell*, **61**, 885–894.
7. Koslowsky, D. J., Bhat, G. J., Perrollaz, A. L., Feagin, J. E. & Stuart, K. (1990). The MURF3 gene of *T. brucei* contains multiple domains of extensive editing and is homologous to a subunit of NADH dehydrogenase. *Cell*, **62**, 901–911.
8. Sturm, N. R. & Simpson, L. (1990). Kinetoplast DNA minicircles encode guide RNAs for editing of cytochrome oxidase subunit III mRNA. *Cell*, **61**, 879–884.
9. Golden, D. E. & Hajduk, S. L. (2005). The 3'-untranslated region of cytochrome oxidase II mRNA functions in RNA editing of African trypanosomes exclusively as a cis guide RNA. *RNA*, **11**, 29–37.
10. Stuart, K. D., Schnaufer, A., Ernst, N. L. & Panigrahi, A. K. (2005). Complex management: RNA editing in trypanosomes. *Trends Biochem. Sci.* **30**, 97–105.
11. Aphasizhev, R. & Aphasizheva, I. (2008). Terminal RNA uridylyltransferases of trypanosomes. *Biochim. Biophys. Acta*, **1779**, 270–280.
12. Rusche, L. N., Cruz-Reyes, J., Piller, K. J. & Sollner-Webb, B. (1997). Purification of a functional enzymatic editing complex from *Trypanosoma brucei* mitochondria. *EMBO J.* **16**, 4069–4081.
13. Simpson, L., Aphasizhev, R., Lukes, J. & Cruz-Reyes, J. (2010). Guide to the nomenclature of kinetoplastid RNA editing: a proposal. *Protist*, **161**, 2–6.
14. Trotter, J. R., Ernst, N. L., Carnes, J., Panicucci, B. & Stuart, K. (2005). A deletion site editing endonuclease in *Trypanosoma brucei*. *Mol. Cell*, **20**, 403–412.
15. Carnes, J., Trotter, J. R., Ernst, N. L., Steinberg, A. & Stuart, K. (2005). An essential RNase III insertion editing endonuclease in *Trypanosoma brucei*. *Proc. Natl Acad. Sci. USA*, **102**, 16614–16619.
16. Carnes, J., Trotter, J. R., Peltan, A., Fleck, M. & Stuart, K. (2008). RNA editing in *Trypanosoma brucei* requires three different editosomes. *Mol. Cell Biol.* **28**, 122–130.
17. Panigrahi, A. K., Ernst, N. L., Domingo, G. J., Fleck, M., Salavati, R. & Stuart, K. D. (2006). Compositionally and functionally distinct editosomes in *Trypanosoma brucei*. *RNA*, **12**, 1038–1049.
18. Schnaufer, A., Ernst, N. L., Palazzo, S. S., O'Rear, J., Salavati, R. & Stuart, K. (2003). Separate insertion and deletion subcomplexes of the *Trypanosoma brucei* RNA editing complex. *Mol. Cell*, **12**, 307–319.
19. Kang, X., Gao, G., Rogers, K., Falick, A. M., Zhou, S. & Simpson, L. (2006). Reconstitution of full-round uridine-deletion RNA editing with three recombinant proteins. *Proc. Natl Acad. Sci. USA*, **103**, 13944–13949.
20. Rogers, K., Gao, G. & Simpson, L. (2007). Uridylate-specific 3' 5'-exoribonucleases involved in uridylate-deletion RNA editing in trypanosomatid mitochondria. *J. Biol. Chem.* **282**, 29073–29080.
21. Aphasizhev, R., Sbciego, S., Peris, M., Jang, S. H., Aphasizheva, I., Simpson, A. M. *et al.* (2002). Trypanosome mitochondrial 3' terminal uridylyl transferase (TUTase): the key enzyme in U-insertion/deletion RNA editing. *Cell*, **108**, 637–648.
22. Adler, B. K., Harris, M. E., Bertrand, K. I. & Hajduk, S. L. (1991). Modification of *Trypanosoma brucei* mitochondrial rRNA by posttranscriptional 3' polyuridine tail formation. *Mol. Cell Biol.* **11**, 5878–5884.
23. Aphasizheva, I. & Aphasizhev, R. (2010). RET1-catalyzed uridylylation shapes the mitochondrial transcriptome in *Trypanosoma brucei*. *Mol. Cell Biol.* **30**, 1555–1567.
24. Decker, C. J. & Sollner-Webb, B. (1990). RNA editing involves indiscriminate U changes throughout precisely defined editing domains. *Cell*, **61**, 1001–1011.
25. Etheridge, R. D., Aphasizheva, I., Gershon, P. D. & Aphasizhev, R. (2008). 3' Adenylation determines mRNA abundance and monitors completion of RNA editing in *T. brucei* mitochondria. *EMBO J.* **27**, 1596–1608.
26. Aphasizheva, I., Ringpis, G. E., Weng, J., Gershon, P. D., Lathrop, R. H. & Aphasizhev, R. (2009). Novel TUTase associates with an editosome-like complex in mitochondria of *Trypanosoma brucei*. *RNA*, **15**, 1322–1337.
27. Drozd, M., Palazzo, S. S., Salavati, R., O'Rear, J., Clayton, C. & Stuart, K. (2002). TbMP81 is required for RNA editing in *Trypanosoma brucei*. *EMBO J.* **21**, 1791–1799.
28. Ernst, N. L., Panicucci, B., Igo, R. P., Jr., Panigrahi, A. K., Salavati, R. & Stuart, K. (2003). TbMP57 is a 3' terminal uridylyl transferase (TUTase) of the *Trypanosoma brucei* editosome. *Mol. Cell*, **11**, 1525–1536.
29. Aphasizhev, R., Aphasizheva, I. & Simpson, L. (2003). A tale of two TUTases. *Proc. Natl Acad. Sci. USA*, **100**, 10617–10622.
30. Deng, J., Ernst, N. L., Turley, S., Stuart, K. D. & Hol, W. G. (2005). Structural basis for UTP specificity of RNA editing TUTases from *Trypanosoma brucei*. *EMBO J.* **24**, 4007–4017.
31. Stagno, J., Aphasizheva, I., Aphasizhev, R. & Luecke, H. (2007). Dual role of the RNA substrate in selectivity and catalysis by terminal uridylyl transferases. *Proc. Natl Acad. Sci. USA*, **104**, 14634–14639.
32. Igo, R. P., Palazzo, S. S., Burgess, M. L., Panigrahi, A. K. & Stuart, K. (2000). Uridylate addition and RNA ligation contribute to the specificity of kinetoplastid insertion RNA editing. *Mol. Cell Biol.* **20**, 8447–8457.
33. Aphasizhev, R., Aphasizheva, I., Nelson, R. E., Gao, G., Simpson, A. M., Kang, X. *et al.* (2003). Isolation of a U-insertion/deletion editing complex from *Leishmania tarentolae* mitochondria. *EMBO J.* **22**, 913–924.
34. Igo, R. P., Jr., Lawson, S. D. & Stuart, K. (2002). RNA sequence and base pairing effects on insertion editing in *Trypanosoma brucei*. *Mol. Cell Biol.* **22**, 1567–1576.
35. Aphasizhev, R. & Aphasizheva, I. (2007). RNA editing uridylyltransferases of trypanosomatids. *Methods Enzymol.* **424**, 51–67.
36. Larsen, L. S., Wassman, C. D., Hatfield, G. W. & Lathrop, R. H. (2008). Computationally optimised DNA assembly of synthetic genes. *Int. J. Bioinform. Res. Appl.* **4**, 324–336.
37. Wirtz, E., Leal, S., Ochatt, C. & Cross, G. A. (1999). A tightly regulated inducible expression system for conditional gene knock-outs and dominant-negative genetics in *Trypanosoma brucei*. *Mol. Biochem. Parasitol.* **99**, 89–101.

38. Sloof, P., Bos, J. L., Konings, A. F., Menke, H. H., Borst, P., Gutteridge, W. E. & Leon, W. (1983). Characterization of satellite DNA in *Trypanosoma brucei* and *Trypanosoma cruzi*. *J. Mol. Biol.* **167**, 1–21.
39. Wickstead, B., Ersfeld, K. & Gull, K. (2002). Targeting of a tetracycline-inducible expression system to the transcriptionally silent minichromosomes of *Trypanosoma brucei*. *Mol. Biochem. Parasitol.* **125**, 211–216.
40. Puig, O., Caspary, F., Rigaut, G., Rutz, B., Bouveret, E., Bragado-Nilsson, E. *et al.* (2001). The tandem affinity purification (TAP) method: a general procedure of protein complex purification. *Methods*, **24**, 218–229.
41. Jensen, B. C., Kifer, C. T., Brekken, D. L., Randall, A. C., Wang, Q., Drees, B. L. & Parsons, M. (2007). Characterization of protein kinase CK2 from *Trypanosoma brucei*. *Mol. Biochem. Parasitol.* **151**, 28–40.
42. Kelly, S., Reed, J., Kramer, S., Ellis, L., Webb, H., Sunter, J. *et al.* (2007). Functional genomics in *Trypanosoma brucei*: a collection of vectors for the expression of tagged proteins from endogenous and ectopic gene loci. *Mol. Biochem. Parasitol.* **154**, 103–109.
43. Stagno, J., Aphasizheva, I., Rosengarth, A., Luecke, H. & Aphasizhev, R. (2007). UTP-bound and Apo structures of a minimal RNA uridylyltransferase. *J. Mol. Biol.* **366**, 882–899.
44. Aphasizheva, I., Aphasizhev, R. & Simpson, L. (2004). RNA-editing terminal uridylyl transferase 1: identification of functional domains by mutational analysis. *J. Biol. Chem.* **279**, 24123–24130.
45. Schnauffer, A., Wu, M., Park, Y. J., Nakai, T., Deng, J., Proff, R. *et al.* (2010). A protein-protein interaction map of trypanosome ~20S editosomes. *J. Biol. Chem.* **285**, 5282–5295.
46. Holm, L. & Sander, C. (1995). DNA polymerase beta belongs to an ancient nucleotidyltransferase superfamily. *Trends Biochem. Sci.* **20**, 345–347.
47. Beard, W. A. & Wilson, S. H. (2006). Structure and mechanism of DNA polymerase beta. *Chem. Rev.* **106**, 361–382.
48. Prasad, R., Beard, W. A. & Wilson, S. H. (1994). Studies of gapped DNA substrate binding by mammalian DNA polymerase beta. Dependence on 5'-phosphate group. *J. Biol. Chem.* **269**, 18096–18101.
49. Ochsenreiter, T., Cipriano, M. & Hajduk, S. L. (2007). KISS: the kinetoplastid RNA editing sequence search tool. *RNA*, **13**, 1–4.
50. Kang, X., Rogers, K., Gao, G., Falick, A. M., Zhou, S. & Simpson, L. (2005). Reconstitution of uridine-deletion precleaved RNA editing with two recombinant enzymes. *Proc. Natl Acad. Sci. USA*, **102**, 1017–1022.
51. Weng, J., Aphasizheva, I., Etheridge, R. D., Huang, L., Wang, X., Falick, A. M. & Aphasizhev, R. (2008). Guide RNA-binding complex from mitochondria of trypanosomatids. *Mol. Cell*, **32**, 198–209.
52. Pelletier, M., Read, L. K. & Aphasizhev, R. (2007). Isolation of RNA binding proteins involved in insertion/deletion editing. *Methods Enzymol.* **424**, 69–96.